Taylor & Francis
Taylor & Francis Group

Journal of Microencapsulation
Micro and Nano Carriers

ISSN: 0265-2048 (Print) 1464-5246 (Online) Journal homepage: http://www.tandfonline.com/loi/imnc20

Magnetic Nanogel Polymer of Bupivacaine for Ankle Block in Rats

Sadigheh Nadri, Hormoz Mahmoudvand & Ali Eatemadi

To cite this article: Sadigheh Nadri, Hormoz Mahmoudvand & Ali Eatemadi (2016): Magnetic Nanogel Polymer of Bupivacaine for Ankle Block in Rats, Journal of Microencapsulation, DOI: 10.1080/02652048.2016.1242667

To link to this article: http://dx.doi.org/10.1080/02652048.2016.1242667

Accepted author version posted online: 28 Sep 2016.

Magnetic Nanogel Polymer of Bupivacaine for Ankle Block in Rats

Authors:

Sadigheh Nadri[1], Hormoz Mahmoudvand[2*], Ali Eatemadi[3*]

Affiliations:

[1]Department of anesthesiology, Lorestan University of Medical sciences, Khoramabad, Iran

[2]Department of Surgery, Lorestan University of Medical sciences, Khoramabad, Iran

[3]Department of Medical Biotechnology, School of advance Science in Medicine, Tehran University of Medical sciences, Tehran, Iran

Corresponding author:

Hormoz Mahmoudvand, Department of Surgery, Lorestan University of Medical sciences, Khoramabad, Iran. Tele/fax: +982166423101, Postal address: 13185-1678, EMAIL: Ali.eatemadi18@gmail.com and Ali Eatemadi, Department of Medical Biotechnology, School of advance Science in Medicine, Tehran University of Medical sciences, Tehran, Iran, Tel/fax: +989188426723, Postal address: 69971-18544, E-MAIL: a-eatemadi@razi.tums.ac.ir.

Abstract

Introduction: In an effort of designing an alternative method for local nerve block, we demonstrated the possibility of inducing ankle block in the rat with intravenous (IV) injection of magnetic nanoparticles conjugated bupivacaine and application of a magnet at the ankle.

Methods: The anesthetic effect of magnet-directed bupivacaine-associated MNPs (NIPAAM-MAA-bupivacaine) was tested in rat using paw withdrawal latencies from thermal stimuli on the hindpaw. Thirteen (13) experimental animals were grouped into two; untreated left hindpaw (control group), and test group with treated right hindpaw. The morphology of the synthesized nanogel was analysed using surface electron micrograph (SEM), chemical characterization using FTIR and NMR, and finally the *in vivo* drug release using UV spectroscopy.

Results: UV Spectroscopy result show that, at 37°C a sharp increase was observed from 24-72h (40-75%) cumulative drug release at pH 5.3, a steady increase from 21-60% and 20-40% at pH 6.8 and 7.4 respectively. At 43°C a steady increase was observed at the three pH, 37-72%, 20-35% and 10-19% at pH 5.3, 6.8 and 7.4 respectively. It was shown also that drug release at higher pH (6.8 and 7.4) does not become significantly faster when temperature is high, compared to the release at a pH of 5.3. This depicts that the decreasing pH has more impact on the speed of the release of drug than increasing temperature. NMR and FTIR results displayed a comparable chemical structure as expected. The NMR peak displayed high purity of the final product. Morphology using SEM showed that the nanocomposite size is slightly greater than that of the nanogel, and the nanocomposite particles are nearly mono dispersed. Paw withdrawal latency highest peak of 15% was observed for NG/PU/30 at 40hours, and lowest peak for NG/30 at 50hours for the left paw. Group BU0.15 at 30hours shows the highest peak (20%) and NG/30 at 120h shows the lowest peak for the right treated paw, which is significantly difference from the untreated left paw group ($P < 0.0001$). However, there wasn't a significant difference amongst NG/30, NG/Pub/15, or NG/Pub/60.

Conclusions: The current study verifies the findings that we can induce ankle block in rat through IV injection administration of NIPAAM-MAA-bupivacaine complexes and the application of magnet at the ankle. We however suggest a lower temperature and pH for optimum release of this nanoanesthetics, there is a probability of translating this mechanism to clinical practice.

Keywords: Nanogel; Magnetic nanoparticles; Anesthesia; Ankle block; Bupivacaine

1 Introduction

Chemotherapeutic agents targeted delivery coupled with magnetic nanoparticles (MNPs) has been favorably illustrated in animals (Widder *et al.* 1981, Pulfer and Gallo 1998, Alexiou *et al.* 2000, Haisch *et al.* 2002) and humans. (Lübbe *et al.* 1996) MNPs are complexes attractable by a magnet, and could be probably find applications in directing anesthetic drugs to a particular tissue. Moreover, MNPs like those used in the present study are constant in aqueous solution below a particular temperature but diminish and discharge any drug loaded on them at higher temperatures. (Adabi *et al.* 2016) These two characteristics allow drug-associated MNPs to be administered IV and for the MNPs to be sequestered and concentrated with magnets in a superficial tissue where the drug is released at body temperature to have an effect in the tissue.

NIPAAm-MAA conjugated curcumin has been employed in molecular biology, it exerted cytotoxic effects on the Calu-6 cell line via down-regulation of telomerase and induction of pinX1 gene expression. NIPPAm-MAA has been said to be a potential carrier for such types of hydrophobic agent (Badrzadeh *et al.* 2014). Poly (N-isopropylacrylamide) (PNIPAAm) the widely known thermosensitive polymer, could release drug in a somewhat acidic medium, which occurs in, solid tumors, inflammatory tissues, and intracellular endosomal compartment (Badrzadeh *et al.* 2014).

The aim of this study was to verify if magnetic-nanogel directed targeting of the frequently utilize local anesthetic drug bupivacaine associated with MNPs is capable of inducing anesthetic ankle block in the rat. Bupivacaine -associated NIPAAM-MAA complexes were injected IV attracting them to a magnet

applied at the ankle. The mechanism behind this was that when the complexes in circulation gets to the ankle, they would be sequestered and concentrated there, the bupivacaine would be released locally, and then act on the nerves surrounding the ankle, and brings about anesthetic block.

2 Methods

2.1 Preparation of NIPAAM-MAA Complexes

We applied free radical emulsion polymerization method to synthesize this nanogel. NIPAAM and MAA were scattered in water in a molar ratio of 70 to 30 respectively. BIS serve as a cross-linker. SDS being the surfactant agent used at a ratio of 3% of monomer weight.(Aiyelabegan *et al.* 2016, Beiranvand *et al.* 2016) To start the process of polymerization, potassium per sulfate (KPS) was used as the initiating agent (at a ratio of 3.5% weight of monomers). Thirty minutes (30mins) after degassing the mixed solution with N2, the increment in temperature of the mixture approaches 70 ° C, then the initiator was permitted to be poured into it slowly.(Daraee, Eatemadi, *et al.* 2016, Daraee, Etemadi, *et al.* 2016) Polymerization process continued for 4h at this temperature, after which the polymer solution (latex) was cooled. Dialysis bag membrane was used to purify the synthesized against distilled water for 5 days. Excess synthesized polymer was freeze-dried and stored for further experiments (Kaveh Kurd, Amir Ahmad Khandagi, Soodabeh Davaran 2015).

2.2 Preparation of Bupivacaine-loaded magnetic hydrogel nanocomposite

Bupivacaine-loaded magnetic hydrogel nanocomposite was synthesized by dissolving the hydrogel in a solution of NaOH in the presence of Bupivacaine and magnetic nanoparticles (MNPs).(Eatemadi, Darabi, *et al.* 2016, Ghafarzadeh *et al.* 2016) We dispersed 100mg of MNPs and 50mg of Bupivacaine in 40ml of 25mM NaOH solution, followed by sonication at a 0.5 cycle and 50% amplitude for 15 min. The temperature of the solution increased to 50°C. Consequently, 400mg of freeze-dried nanogel was scattered in the solution and then sonicated again at the above-mentioned conditions for 5 min. The solution was allowed to stand for 48h in a shaking incubator at 5°C, to allow for nanogel groove formation, and the encapsulation of Bupivacaine and MNPs into it. The next stage involves the

centrifugation of the solution, the supernatant was separated and precipitated. The nanocomposite was washed with NaOH, dialyzed against deionized water for a period of 3 days, to expel free Bupivacaine and NaOH. The dialyzed solution was centrifuged, freeze-dried and kept for subsequent research (Mantha *et al.* 2014).

2.3 Measurement of Drug-loading and encapsulation efficiency

We used this relationship to evaluate the percentage of Bupivacaine encapsulated on the nanoparticles (EE) (Equation 1) and drug loading (DL) (Equation 2) was measured(Eatemadi *et al.* 2014, Eatemadi, Daraee, *et al.* 2016):

EE= (Weight of Loaded Bupivacaine / Weight of the initial Bupivacaine) X 100% (Equation 1)

DL= (Weight of Loaded Bupivacaine / Weight of the Nanoparticles) X 100% (Equation 2)

2.4 Morphological study

Morphological properties such as shape, and size, of the nanocomposite and nanogel synthesized were observed by SEM (VEGA, TESCAN, Czech Republic). A drop of nanocomposite and nanogel were placed on aluminum foil and allowed to dry. After coating, the sample was then viewed under 10kV SEM.

Polydispersity index (PDI) of the nanocomposite and nanogel was measured by Gel Permeation Chromatograph (GPC) using a Waters 515 Differential Refactometer with Waters 410 HPLC pump and two styrage HR 5E columns in THF (0.1 mg/L) as an eluent at 42 °C, calibrated with polystyrene standards. The PDI values range from 1.0 to 1.1; a higher value indicates a less homogeneous NP size distribution.

PDI from GPC =Mw/Mn

2.5 Chemical characterization

Hydrogel and drug-loaded nanocomposite characterization was carried out by Fourier Transform Infrared (FTIR) spectroscopy with the KBr disk. We dispersed the nanogel in a solution of dimethyl sulfoxide (DMSO) and followed by its characterization with NMR spectroscopy.

2.6 Animal experiments

We obtained approval for animal experiments from the Ethical Committee of Lorestan University of Medical Sciences. Male rats were used for the ankle block experiments (n=8, 330-360g) and the pharmacokinetic studies (n=5; 360–390g). Rats were taken care of in conformity with the IACUC regulations. The study adheres to the Use of Laboratory Animals and the Guide for the Care and Use of Laboratory Animals (1996).

2.7 Animal exposure

The animals were first anesthesized under 2% isoflurane in oxygen with spontaneous ventilation, and magnets placed around the ankle of the right hindpaw. The left hindpaw represent the untreated control group without magnet application. Then, Bupivacaine was administered in five injections to the ankle, using the malleoli as landmarks. Prior to injection administration, the magnetic loaded Bupivacaine complexes were removed from the ice container used for transport and was left to warm between 10°C to 15°C to avert probable ventricular fibrillation (Mantha *et al.* 2014).

The magnetic loaded Bupivacaine nanogels (or magnet nanogels alone) were then manually administered through the cannula over 4 to 5 minutes by the same researcher. Considering the fact that nearly 10% or less of the administered dose would be sequestered and present at the ankle, we administered 2mL magnetic loaded Bupivacaine suspension (containing 14 mg Bupivacaine or 40–46 mg/kg). Three groups of mice magnets were removed after 15, 30, or 60 minutes, respectively. For the nanogels alone vehicle (NG30), the magnet was removed after 30 minutes. The effect of magnet-directed concentration of the magnetic loaded bupivacaine was juxtaposed with the effect of conventional ankle block with 0.15% Bupivacaine, which served as benchmarks. This method is a

slight modification of Mantha et al., 2014 (Mantha *et al.* 2014).

2.8 Assessment of Ankle Block

Anesthesia was evaluated through the well-established method by Hargreaves et al. (Hargreaves *et al.* 1988), plantar thermal nociception assay and the IITC Plantar Test Analgesia Meter (IITC, Woodland Hills, CA). Prior to anesthetic administration, animals were subjected to individual acrylic testing chambers on a raised glass platform in a dimly lit, quiet room and tested for baseline sensitivity to radiant thermal stimuli focused on the plantar surface of the hindpaw from below.(Mellatyar *et al.* 2014, Ghafarzadeh *et al.* 2016)

2.9 Animals and paw withdrawal latency testing

After purchase, all rats were housed at room temperature (20–25°C) under a 12h light and 12h dark cycle with accessibility to water and food ad libitum. Thermal hyperalgesia thresholds were determined as explained earlier in the literature (Hargreaves *et al.* 1988). Rat were fixed on a preheated glass platform in a plastic chamber. After the rat was acclimatized to the plexiglass chamber in a Hargreaves apparatus (Model 37370, Ugo-Basile, Comerio, Italy), the plantar surface of concerned hind paw was subjected to a beam of radiant heat via a transparent perspex surface. Paw withdrawal latency (PWL) to the radiant heat stimulus was documented with the infrared intensity set at 50%, cut-off time 15s, and reaction time 0.1s. The heat stimulation was repeated 3 times at an interval of 2–3 min for each paw and the averages were then computed. All rats were conditioned to the paw withdrawal chambers 1h daily and we evaluated PWL to heat stimulation values on both the operative and control paws 2 days before surgery. The average value of five measures was recorded as the baseline value (An *et al.* 2015).

2.10 *In vitro*-release studies

The in vitro drug release involve six different sets of experiments performed. These included two temperatures (37°C and 43°C) and three pH levels (5.3, 6.8 and 7.4). For each of the drug-release experiment, 3.0 mg of the drug carrier bonded with smart polymer was sealed in a 30 mL of Na_2HPO_4-

NaH_2PO_4 solution of buffer at a pH of 5.3, 6.8 or 7.4. The test tube with a cork was placed in a water bath and maintained at 43°C up to the lower critical solution temperature or 37°C. The release medium (about 3 mL) was withdrawn at predetermined time intervals (and 336 hours). The samples were then analyzed using an ultraviolet-visible spectrometer to analyze the amount of Bupivacaine released.

Percentage drug release is calculated using the expression below;

$$\text{Drug release (\%)} = \frac{\text{Released Drug}}{\text{Total drug}} \times 100$$

2.11 Statistical Analysis

Statistical analysis was carried out using GraphPad Prism 5.01 (San Diego, CA, USA) through a repeated-measures one-way analysis of variance (ANOVA) followed by the Bonferroni's multiple comparison test or two-way ANOVA followed by Bonferroni's post-tests for determining the effects of dose, time, and dose by time on PWL. The statistical significance was estimated as $P< 0.05$. All data were presented as means ± standard error of mean.

3 Results

3.1 Chemical structure of NIPAAM-MAA

Figure 1 (A) shows the FTIR spectrum of the nanogel synthesized. The peaks at 1650 cm^{-1} and 1690 cm^{-1} represents the stretching carbonyl NIPAAM group. The peak at 1730 cm^{-1} represents the C-O carbonyl group stretch of the ester bond. The C–C backbone stretching is seen at 800–1000 cm^{-1}. The peak at 1717 cm^{-1} represents the carboxylic group of MAA.(Seidi *et al*. 2014, Mohammadian and Eatemadi 2016).

(B) presents the FTIR spectrum of the Bupivacaine-loaded nanocomposite synthesized. The peaks are nearly matched, except for the diminishing peak that was characteristics of MAA carboxylic group. This event represents the conjugation between MAA and OH of the carboxylic group.

Figure 2 represents the NMR spectrum of the nanogel. The terminal isopropyl methyl protons show a high peak at 1.1ppm. The peak at 3.8ppm represents isopropyl methylene protons. The MAA protons

carboxylic group is shown in a weak peak at 12ppm. Nanogel backbone methylene protons were shown at 1.3–2.2 ppm. The amide N–H group's peak was also shown at 8.1–8.2 ppm. This NMR and FTIR result displayed a comparable chemical structure as expected. The NMR peak displayed the high purity of the final product.

3.2 Morphological study

Figure 3 shows the SEM micrograph of the nanogel (A) and the Bupivacaine-loaded nanocomposite (B). As it has been shown, the nanocomposite mean particle size is 52 nm, particle size distribution, PDI is 1.0100) is slightly greater than that of the nanogel mean particle size is 48 nm, particle size distribution, PDI is 1.0018). (Table 1) This could be related to the fact that some of the MNPs are absorbed on the surface of the nanogel and the interaction between their surface charges acts as a signal for assembling the nanocomposite, and its increase in size. Micrograph of the nanocomposite depicts that the particles are nearly mono dispersed. These characteristics is crucial for MNPs application in hyperthermia, to generate more heat equivalent to the applied magnetic field.

3.3 *In vitro* drug release from the Bupivacaine-loaded composite nanoparticles

Figure 4 show drug release from the composite nanoparticle, over 336h time interval at a temperature of 37°C and 43°C, at 37°C (A) a sharp increase was observed from 24-72h (40-75%) cumulative drug release at pH 5.3, a steady increase from 21-60% and 20-40% at pH 6.8 and 7.4 respectively. At 43°C (B) a steady increase was observed at the three pH, 37-72%, 20-35% and 10-19% at pH 5.3, 6.8 and 7.4 respectively. This shows that bupivacaine drug release at higher pH (6.8 and 7.4) does not become significantly faster when temperature is high, compared to the release at a pH of 5.3, the decreasing pH has more impact on the speed of the release of drug than increasing temperature.

3.4 Duration of sensory nerve block

The raw data for withdrawal latencies for each of the treatment groups were plotted independently for the untreated and treated paws. Figure 5 characterizes the variability at each time point by plotting the lower halves of the 95% CIs. The mixed effects model was also used to test the outcome of paired

differences between the untreated left and treated right paws. The highest peak of 15% was observed for NG/PU/30 at 40hours, and lowest peak for NG/30 at 50hours for the left paw. Group BU0.15 at 30hours shows the highest peak (20%) and NG/30 at 120h shows the lowest peak for the right treated paw, which is significantly difference from the untreated left paw group ($P< 0.0001$). However, there wasn't a significant difference amongst NG/30, NG/Pub/15, or NG/Pub/60 ($P< 0.0001$).

4 Discussion

We induced ankle block via IV injection of NIPAAM-MAA/Bupivacaine complexes with magnetic application at the rat ankle. The synthesized hydrogel magnetic nanoparticles has five main parts: the MAA group, NIPAAM group, cross-linker segment (BIS), HEM group, and the backbone. The MAA carboxylic group of is responsible for conjugation with bupivacaine. MNPs and some of the bupivacaine incorporate in the network of the gel. Physically incorporated bupivacaine seems be released faster than cisplatin conjugated with the carboxylic group of MAA. The results of our UV Spectroscopy show that, at 37°C a sharp increase was observed from 24-72h (40-75%) cumulative drug release at pH 5.3, a steady increase from 21-60% and 20-40% at pH 6.8 and 7.4 respectively. At 43°C a steady increase was observed at the three pH, 37-72%, 20-35% and 10-19% at pH 5.3, 6.8 and 7.4 respectively. It was shown also that drug release at higher pH (6.8 and 7.4) does not become significantly faster when temperature is high, compared to the release at a pH of 5.3. This depicts that the decreasing pH has more impact on the speed of the release of drug than increasing temperature. NMR and FTIR results displayed a comparable chemical structure as expected. The NMR peak displayed high purity of the final product. Morphology using SEM showed that the nanocomposite size is slightly greater than that of the nanogel, and the nanocomposite particles are nearly mono dispersed.

Paw withdrawal latency highest peak of 15% was observed for NG/PU/30 at 40hours, and lowest peak for NG/30 at 50hours for the left paw. Group BU0.15 at 30hours shows the highest peak (20%) and NG/30 at 120h shows the lowest peak for the right treated paw, which is significantly difference from the untreated left paw group ($P< 0.0001$). However, there wasn't a significant difference amongst

NG/30, NG/Pub/15, or NG/Pub/60. Our findings is similar with the study carried out by Mantha et al. (Mantha *et al.* 2014) who establishes proof of mechanism that it is possible to induce rat ankle block by IV injection administration of MNP/Ropivacaine complexes and magnet application at the ankle. Mantha et al.(Mantha *et al.* 2014) studied the possibility of stimulating ankle block in the rat with IV injection of magnetic nanoparticles (MNPs) associated with ropivacaine and application of a magnet at the ankle. Thirty minutes of magnet application to the ankle of animals injected with MNP/Ropiv was more effective than 15 or 60 minutes of magnet application, which correspond with the result of our latent paw withdrawal. This may be explained by the drug release profile of the complexes. (Mantha *et al.* 2014)

Also in a research conducted by An et al. (An *et al.* 2015) dexamethasone was used as an adjuvant to bupivacaine for prolonging the duration of thermal antinociception and prevention of bupivacaine-induced rebound hyperalgesia through regional mechanism in a mouse sciatic nerve block model. They deduced that perineural, not systemic, dexamethasone added to a clinical concentration of bupivacaine may not only extend the duration of motor and sensory blockade of sciatic nerve, but as well impede the bupivacaine-induced reversible neurotoxicity and short-term "rebound hyperalgesia" after nerve block resolution.

A *in vitro* cytotoxicity test conducted by Nejati-Koshki et al. (Nejati-Koshki *et al.* 2014) showed that the Fe3O4-PLGA-PEG6000 magnetic nanoparticles had no cytotoxicity and were biocompatible (Nejati-Koshki *et al.* 2014), cytotoxic effect on the cells was elevated with increasing concentration of NIPAAm-MAA-curcumin conjugates and was dose and time-dependent (Badrzadeh *et al.* 2014).

Local anesthetics have been related with inflammatory response increase, myotoxicity and altered nerve permeability (Selander 1993). Bupivacaine could activate apoptosis in a dose-dependent manner through mitochondrial membrane disruption, caspase 3 activation and other byproducts (Chang *et al.* 2014). Our results show that bupivacaine administered within our study concentrations did not induce significant apoptosis during the study period.

Future research will address limitations of the current study, which include lack of a formal toxicity study of MNP/Bup, a separate experimental group with ankle injections of saline to serve as negative controls, another group with MNP/Bup IV injections without magnet application (although the left paws served this purpose in our study), determination of bupivacaine concentration in the control ankle and in major organs, and histological examination of the ankles and major organs for iron deposition.

5 Conclusion

We have demonstrated a proof of principle that it is possible to generate an ankle block in the rat by IV injection administration of NIPAAM-MAA/bupivacaine complexes and magnet application at the ankle. We however suggest a lower temperature and pH for optimum release of this nanoanesthetics, there is a probability of translating this mechanism to clinical practice.

Acknowledgment

The authors thank the Department of Medical Biotechnology, School of advance Science in Medicine, Tehran University of Medical Sciences and Department of anesthesiology, Lorestan University of Medical sciences, Khoramabad, Iran. This work is funded by the Grant 2015-171355423 of the Lorestan University of Medical Sciences.

Funding: This study was funded by The Research Center Lorestan University of Medical Sciences (grant number 2013-675938193).

Conflict of interest: The authors declare that they have no conflict of interest.

Ethical approval: All applicable international, national, and/or institutional guidelines for the care and use of animals were followed. All procedures performed in studies involving animals were in accordance with the ethical standards of the ethical board of Lorestan University of Medical Sciences.

Informed consent: Informed consent was obtained from all individual participants included in the study.

References

Adabi, M., Naghibzadeh, M., Adabi, M., Zarrinfard, M.A., Esnaashari, S.S., Seifalian, A.M., Faridi-Majidi, R., Tanimowo Aiyelabegan, H., and Ghanbari, H., 2016. Biocompatibility and nanostructured materials: applications in nanomedicine. *Artificial Cells, Nanomedicine, and Biotechnology*, 1401 (June), 1–10.

Aiyelabegan, H.T., Zaidi, S.S.Z., Fanuel, S., Eatemadi, A., Ebadi, M.T.K., and Sadroddiny, E., 2016. Albumin-Based Biomaterial for Lungs Tissue Engineering Applications. *International Journal of Polymeric Materials and Polymeric Biomaterials*, (just-accepted).

Alexiou, C., Arnold, W., Klein, R.J., Parak, F.G., Hulin, P., Bergemann, C., Erhardt, W., Wagenpfeil, S., and Lubbe, A.S., 2000. Locoregional cancer treatment with magnetic drug targeting. *Cancer Research*, 60 (23), 6641–6648.

An, K., Elkassabany, N.M., and Liu, J., 2015. Dexamethasone as adjuvant to bupivacaine prolongs the duration of thermal antinociception and prevents bupivacaine-induced rebound hyperalgesia via regional mechanism in a mouse sciatic nerve block model. *PLoS ONE*, 10 (4).

Badrzadeh, F., Akbarzadeh, A., Zarghami, N., Yamchi, M.R., Zeighamian, V., Tabatabae, F.S., Taheri, M., and Kafil, H.S., 2014. Comparison between effects of free curcumin and curcumin loaded NIPAAm-MAA nanoparticles on telomerase and pinX1 gene expression in lung cancer cells. *Asian Pacific Journal of Cancer Prevention*, 15 (20), 8931–8936.

Beiranvand, S., Eatemadi, A., and Karimi, A., 2016. New Updates Pertaining to Drug Delivery of Local Anesthetics in Particular Bupivacaine Using Lipid Nanoparticles. *Nanoscale Research Letters*, 11 (1), 1–10.

Chang, Y.-C., Hsu, Y.-C., Liu, C.-L., Huang, S.-Y., Hu, M.-C., and Cheng, S.-P., 2014. Local anesthetics induce apoptosis in human thyroid cancer cells through the mitogen-activated protein kinase pathway. *PloS one*, 9 (2), e89563.

Daraee, H., Eatemadi, A., Abbasi, E., Fekri Aval, S., Kouhi, M., and Akbarzadeh, A., 2016. Application of gold nanoparticles in biomedical and drug delivery. *Artificial cells, nanomedicine, and biotechnology*, 44 (1), 410–422.

Daraee, H., Etemadi, A., Kouhi, M., Alimirzalu, S., and Akbarzadeh, A., 2016. Application of liposomes in medicine and drug delivery. *Artificial cells, nanomedicine, and biotechnology*, 44 (1), 381–391.

Eatemadi, A., Darabi, M., Afraidooni, L., Zarghami, N., Daraee, H., Eskandari, L., Mellatyar, H., and Akbarzadeh, A., 2016. Comparison, synthesis and evaluation of anticancer drug-loaded polymeric nanoparticles on breast cancer cell lines. *Artificial cells, nanomedicine, and biotechnology*, 44 (3), 1008–1017.

Eatemadi, A., Daraee, H., Karimkhanloo, H., Kouhi, M., Zarghami, N., Akbarzadeh, A., Abasi, M., Hanifehpour, Y., and Joo, S.W., 2014. Carbon nanotubes: properties, synthesis, purification, and medical applications. *Nanoscale research letters*, 9 (1), 1–13.

Eatemadi, A., Daraee, H., Zarghami, N., Melat Yar, H., and Akbarzadeh, A., 2016. Nanofiber: synthesis and biomedical applications. *Artificial cells, nanomedicine, and biotechnology*, 44 (1), 111–121.

Ghafarzadeh, M., Eatemadi, A., and Fakhravar, Z., 2016. Human amniotic fluid derived mesenchymal stem cells cause an anti-cancer effect on breast cancer cell line in vitro. *Cellular and Molecular Biology*, 2016 (6), 102–106.

Haisch, A., Kläring, S., Gröger, A., Gebert, C., and Sittinger, M., 2002. A tissue-engineering model for the manufacture of auricular-shaped cartilage implants. *European archives of oto-rhino-laryngology : official journal of the European Federation of Oto-Rhino-Laryngological Societies (EUFOS) : affiliated with the German Society for Oto-Rhino-Laryngology - Head and Neck Surgery*, 259, 316–321.

Hargreaves, K., Dubner, R., Brown, F., Flores, C., and Joris, J., 1988. A new and sensitive method for measuring thermal nociception in cutaneous hyperalgesia. *Pain*, 32 (1), 77–88.

Kaveh Kurd, Amir Ahmad Khandagi, Soodabeh Davaran, A.A., 2015. Cisplatin release from dual-responsive magnetic nanocomposites. *Artifi cial Cells, Nanomedicine, and Biotechnology*.

Lübbe, a S., Bergemann, C., Riess, H., Schriever, F., Reichardt, P., Possinger, K., Matthias, M., Dörken, B., Herrmann, F., Gürtler, R., Hohenberger, P., Haas, N., Sohr, R., Sander, B., Lemke, a J., Ohlendorf, D., Huhnt, W., and Huhn, D., 1996. Clinical experiences with magnetic drug targeting: a phase I study with 4'-epidoxorubicin in 14 patients with advanced solid tumors. *Cancer research*, 56 (20), 4686–4693.

Mantha, V.R.R., Nair, H.K., Venkataramanan, R., Gao, Y.Y., Matyjaszewski, K., Dong, H., Li, W., Landsittel, D., Cohen, E., and Lariviere, W.R., 2014. Nanoanesthesia: A novel, intravenous approach to ankle block in the rat by magnet-directed concentration of ropivacaine-associated nanoparticles. *Anesthesia and Analgesia*, 118 (6), 1355–1362.

Mellatyar, H., Akbarzadeh, A., Rahmati, M., Ghalhar, M.G., Etemadi, A., Nejati-Koshki, K., Zarghami, N., and Barkhordari, A., 2014. Comparison of inhibitory effect of 17-DMAG nanoparticles and free 17-DMAG in HSP90 gene expression in lung cancer. *Asian Pac J Cancer Prev*, 15 (20), 8693–8698.

Mohammadian, F. and Eatemadi, A., 2016. Drug loading and delivery using nanofibers scaffolds. *Artificial cells, nanomedicine, and biotechnology*, 1–8.

Nejati-Koshki, K., Mesgari, M., Ebrahimi, E., Abbasalizadeh, F., Fekri Aval, S., Khandaghi, A.A., Abasi, M., and Akbarzadeh, A., 2014. Synthesis and in vitro study of cisplatin-loaded Fe3O4 nanoparticles modified with PLGA-PEG6000 copolymers in treatment of lung cancer. *Journal of microencapsulation*, 31 (8), 815–823.

Pulfer, S.K. and Gallo, J.M., 1998. Enhanced brain tumor selectivity of cationic magnetic polysaccharide microspheres. *J Drug Target*, 6 (3), 215–227.

Seidi, K., Eatemadi, A., Mansoori, B., Jahanban-Esfahlan, R., and Farajzadeh, D., 2014. Nanomagnet-based detoxifying machine: an alternative/complementary approach in HIV therapy. *Journal of AIDS & Clinical Research*, 2014.

Selander, D., 1993. Neurotoxicity of local anesthetics: animal data. *Reg Anesth*, 18 (6 Suppl), 461–468.

Widder, K.J., Morris, R.M., Poore, G., Howard, D.P., and Senyei, a E., 1981. Tumor remission in Yoshida sarcoma-bearing rts by selective targeting of magnetic albumin microspheres containing doxorubicin. *Proceedings of the National Academy of Sciences of the United States of America*, 78 (1), 579–581.

Figure titles and legends

Figure 1. FTIR spectrum of (A) NIPAAM-MAA nanogel, and (B) NIPAAM-MAA drug-loaded magnetic hydrogel nanocomposite.

Figure 2. NMR spectrum of NIPAAM-MAA nanogel.

Figure 3. SEM micrograph of (A) NIPAAM-MAA nanogel, and (B) NIPAAM-MAA drug-loaded magnetic hydrogel nanocomposite.

Figure 4. Cumulative drug release from the magnetic hydrogel nanocomposite at (A) 37 ° C and (B) 43°C.

Figure 5. Diagram of paw withdrawal latencies (PWL) with 95% confidence intervals (Cis). Lower panel shows the treated, right hindpaw, and upper panel indicate the contralateral, untreated, left hindpaw, after different time of administration of nanogel and nanocomposite.

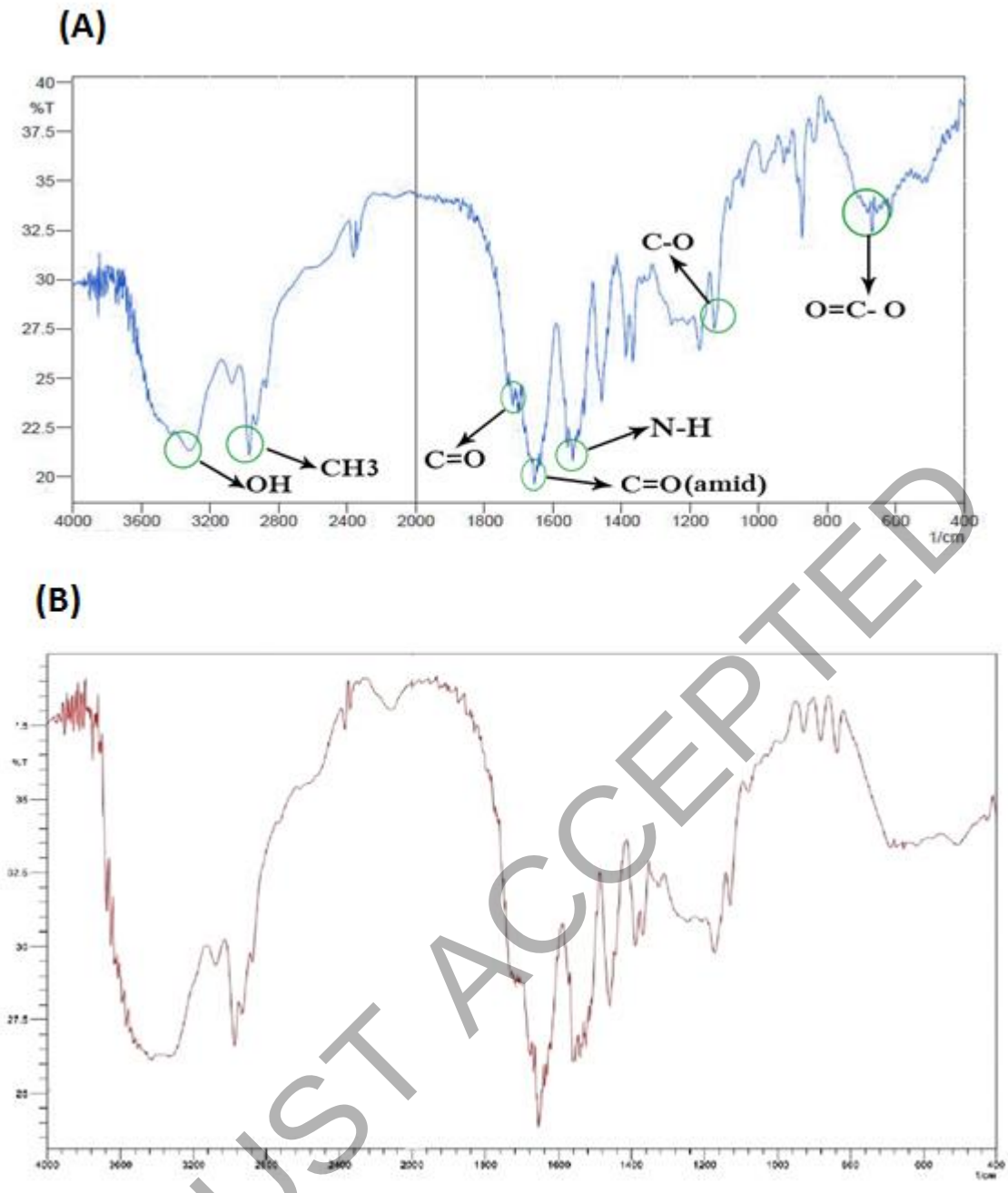

Figure 1. FTIR spectrum showing the stretching of (A) NIPAAM-MAA nanogel synthesized, and (B) NIPAAM-MAA drug-loaded magnetic hydrogel nanocomposite synthesized.

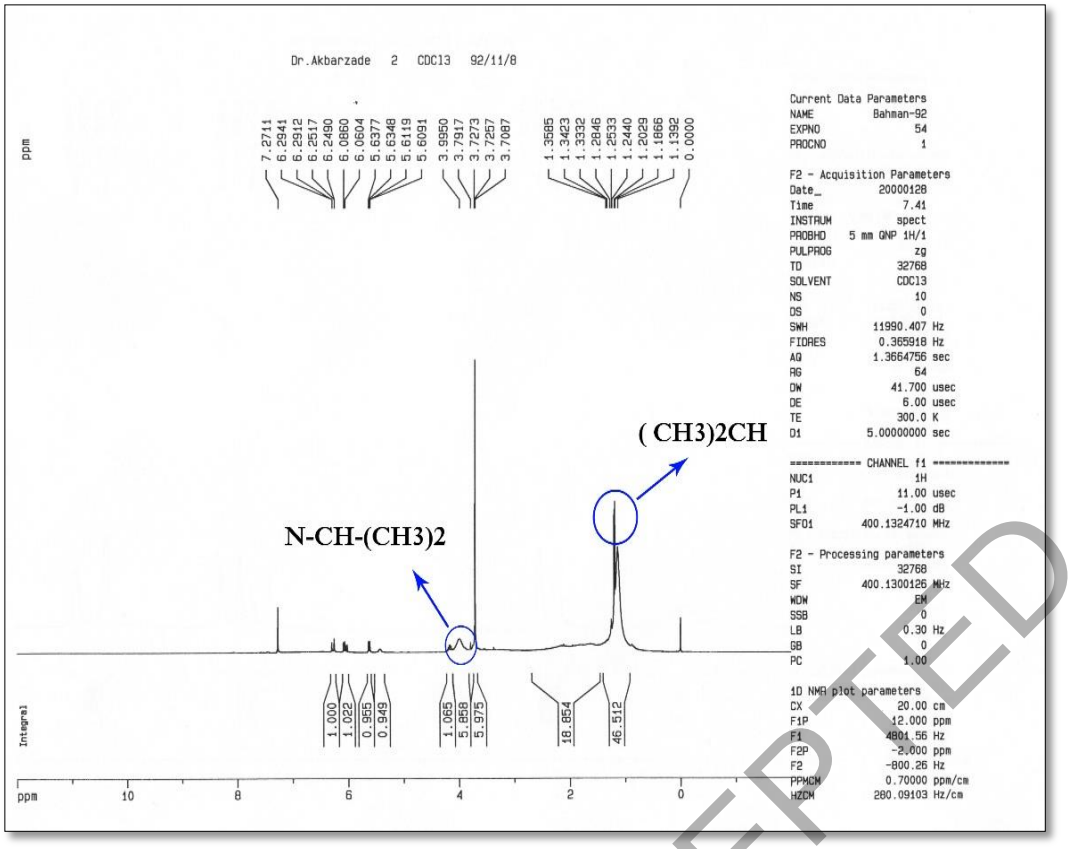

Figure 2. NMR spectrum of the NIPAAM-MAA nanogel. The terminal isopropyl methyl protons showed a high peak at 1.1ppm. The peak at 3.8ppm represents isopropyl methylene protons. MAA protons carboxylic group is shown in a weak peak at 12ppm. Nanogel backbone methylene protons were shown at 1.3–2.2 ppm. The amide N–H group's peak was also shown at 8.1–8.2 ppm, displaying the high purity of the final product.

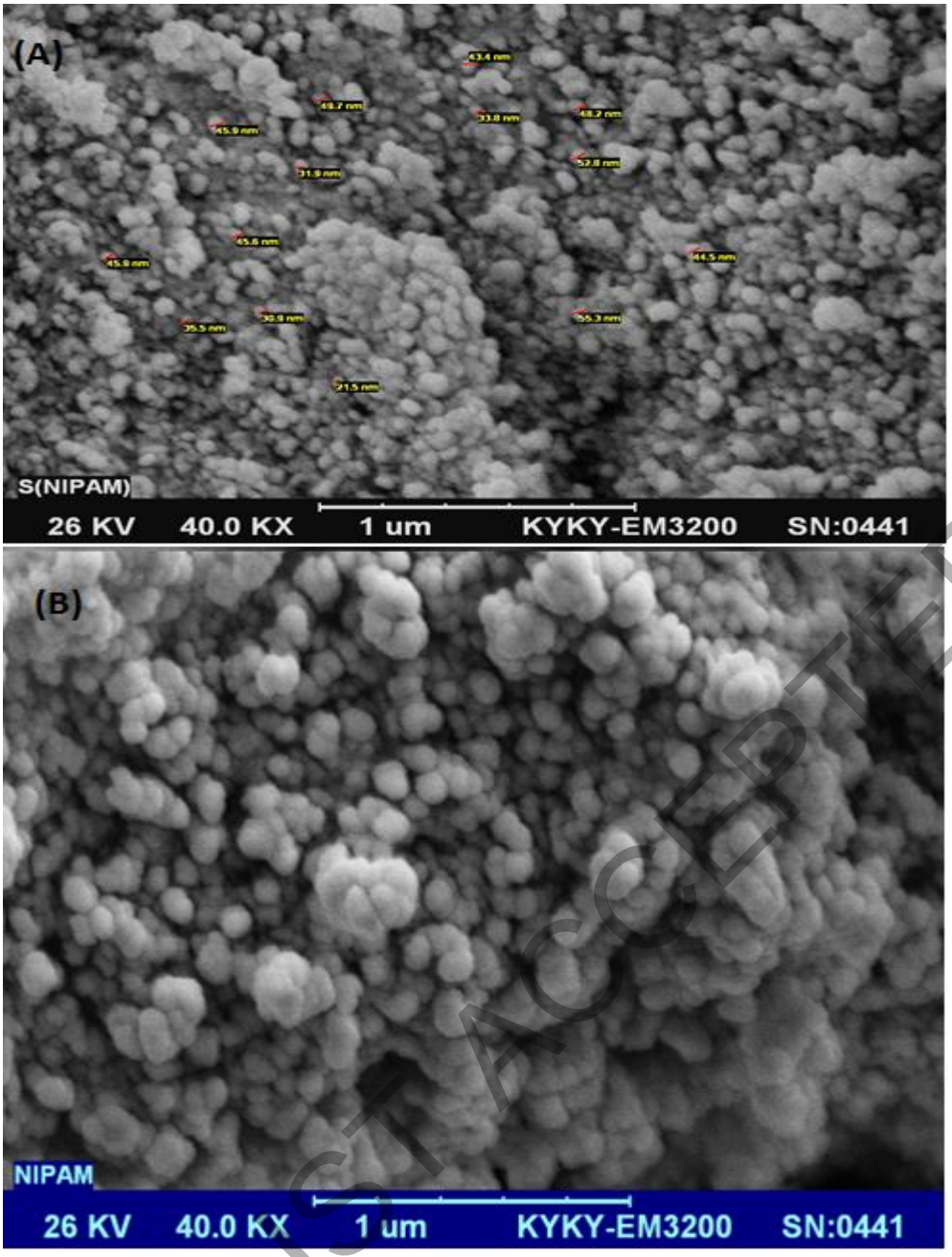

Figure 3. SEM micrograph of (A) NIPAAM-MAA nanogel, and (B) NIPAAM-MAA drug-loaded magnetic hydrogel nanocomposite. The nanocomposite size is slightly greater than that of the nanogel. This could be related to the fact that some of the MNPs are absorbed on the surface of the nanogel and the interaction between their surface charges acts as a signal for assembling the nanocomposite, and its increase in size.

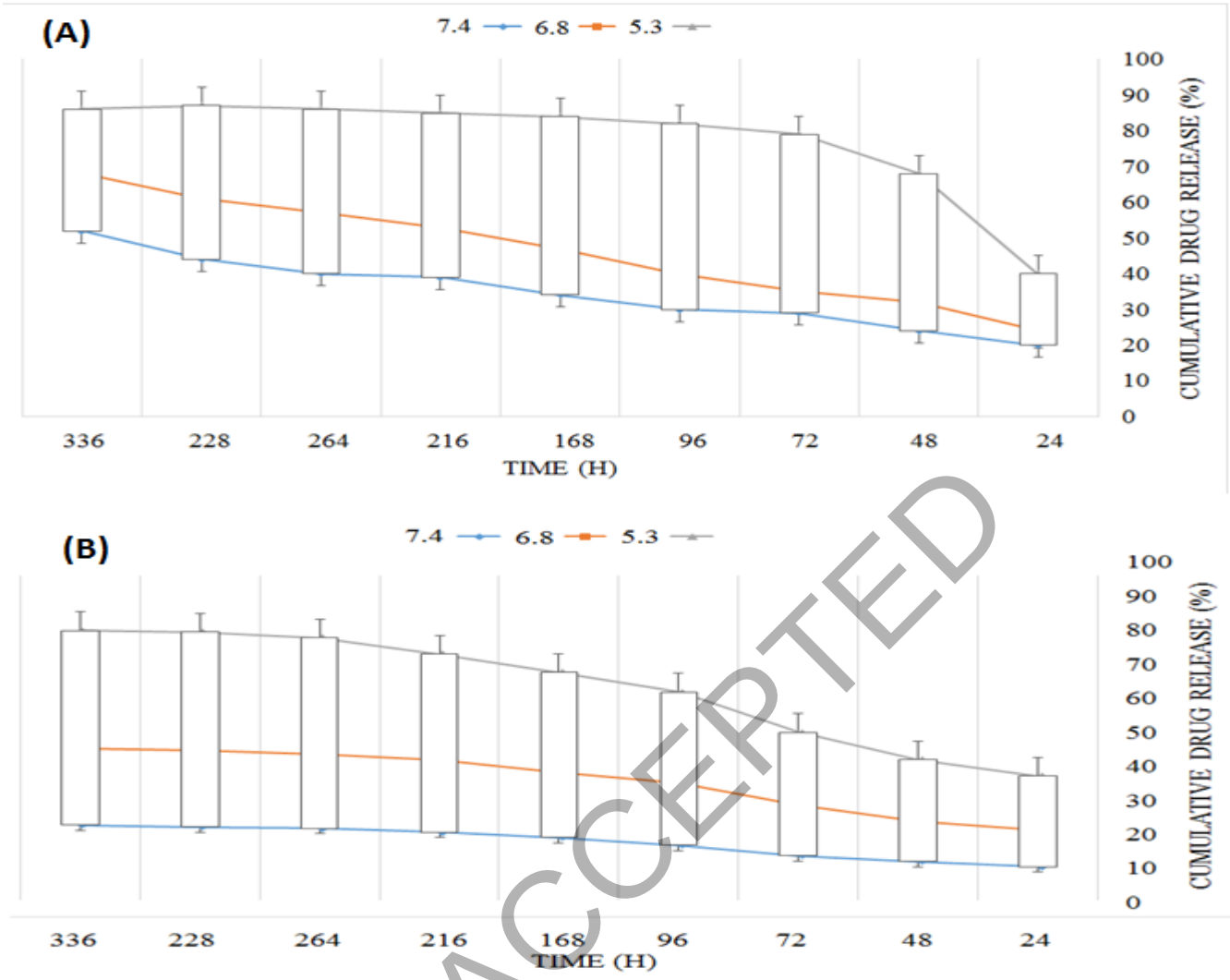

Figure 4. Cumulative release of drug from magnetic hydrogel nanocomposite. Drug release from the composite nanoparticle, over 336h time interval at a temperature of 37°C and 43°C, at 37°C (A) a sharp increase was observed from 24-72h (40-75%) cumulative drug release at pH 5.3, a steady increase from 21-60% and 20-40% at pH 6.8 and 7.4 respectively. At 43°C (B) a steady increase was observed at the three pH, 37-72%, 20-35% and 10-19% at pH 5.3, 6.8 and 7.4 respectively.

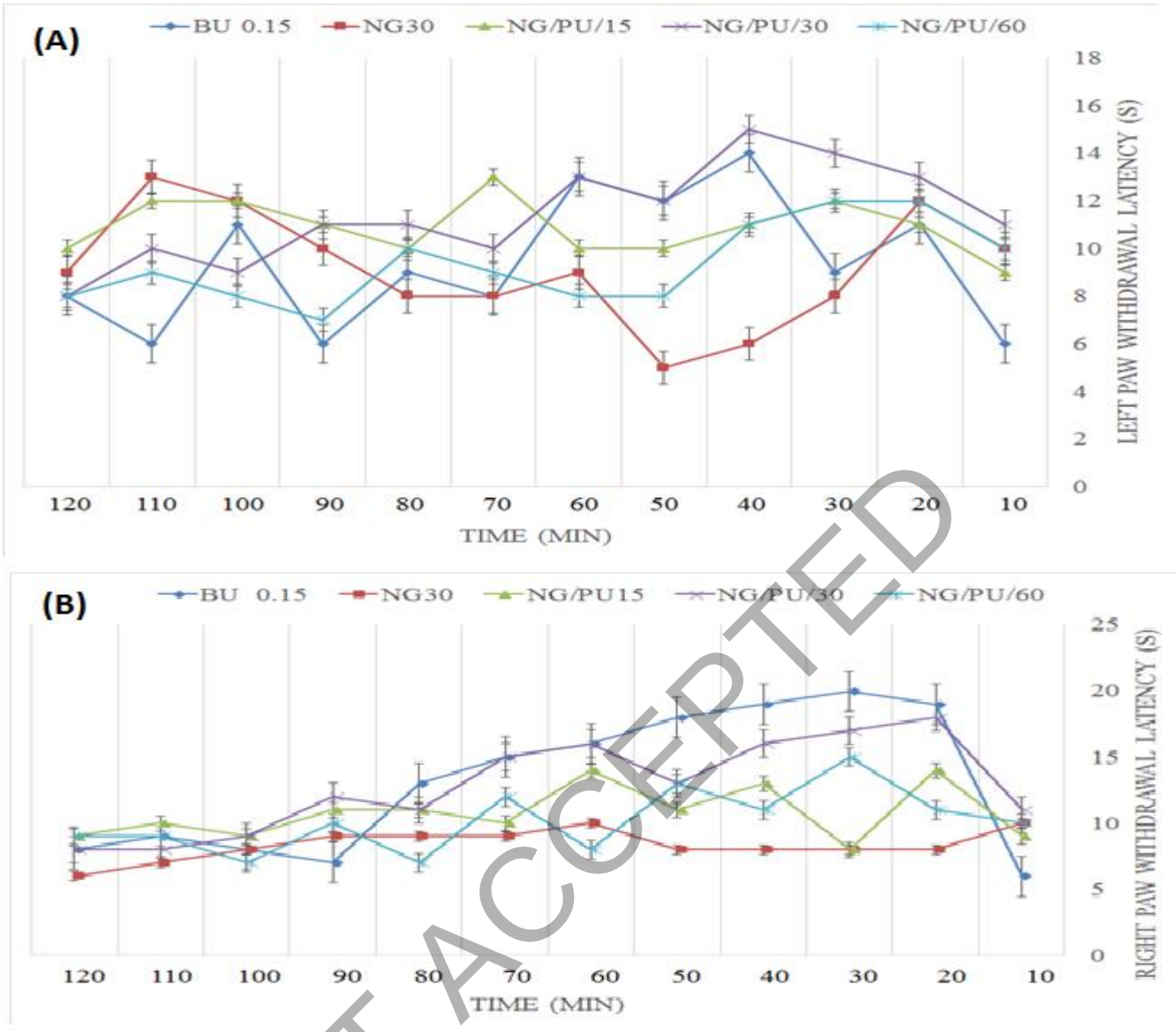

Figure 5. Diagram of paw withdrawal latencies (PWL) with 95% confidence intervals (CIs). A indicate the contralateral, untreated, left hindpaw, and B shows the treated, right hindpaw, after different time of administration of different concentration of nanogel and nanocomposite.

Table 1; PDI of Nanocomposite and nanogel particles prepared

Polymer Name	*Concentration (mol/L)*	M_n	M_w	*PDI*
NIPAAM-MAA	0. 067	109. 2	109. 4	1. 0018
NIPAAM-MAA - bupivacaine	0. 067	130. 0	131. 3	1. 0100

Mw; the mass weighted molecular weight and Mn; the number weighted molecular weight polydispersity determined by gel permeation chromatography (GPC), calibrated with monodisperse polystyrene standards.